

<sup>2</sup>Marko, W. J., "Transonic Dynamic and Static Stability Characteristics of Three Blunt-Cone Planetary Entry Shapes," JPL TR32-1357, Sept. 1969, Jet Propulsion Lab., Pasadena, Calif.

<sup>3</sup>Sammonds, R. I., "Dynamics of High-Drag Probe Shapes at Transonic Speeds," TN D-6489, Sept. 1971, NASA.

<sup>4</sup>Krumins, M. V., "Drag and Stability of Mars Probe/Lander Shapes," *Journal of Spacecraft and Rockets*, Vol. 4, Aug. 1967, pp. 1052-1057.

<sup>5</sup>Cassanto, J. M. and Brice, P., "Free Fall Stability and Base Pressure Drop Tests for Planetary Entry Configurations," *Journal of Spacecraft and Rockets*, Vol. 8, July 1971, pp. 790-793.

<sup>6</sup>Costigan, P. J., "Dynamic-Model Study of Planetary-Entry Configurations in the Langley Spin Tunnel," TND-3499, July 1966, NASA.

<sup>7</sup>Marte, J. E. and Weaver, R. W., "Low-Subsonic Dynamic Stability Investigation of Several Planetary-Entry Configurations in a Vertical Wind Tunnel—Parts I and II," JPL TR-32-743, May 1965, Jet Propulsion Laboratory, Pasadena, Calif.

<sup>8</sup>Short, B. J., "Dynamic Flight Behavior of a Ballasted Sphere at Mach Numbers from 0.4 to 14.5," TN-D-4198, Oct. 1967, NASA.

<sup>9</sup>Seiff, A., Reese, D. E., Sommer, S. C., Kirk, D. B., Whiting, E. E., and Niemann, H. B., "PAET, an Entry Probe Experiment in the Earth's Atmosphere," *Icarus*, Vol. 18, April 1973, pp. 525-563.

## Elevation Stepping of Gimbaled Devices on Rotor-Stabilized Spacecraft

Gerald J. Cloutier\*

M.I.T. Lincoln Laboratory, Lexington, Mass.

### Introduction

THE pointing accuracy of dual-spin or momentum-wheel stabilized spacecraft can be affected by gimbaled sensors which perform scanning motions. These motions can induce nutation of the vehicle. Particularly in cases involving rapid elevation steps in the motion of gimbaled sensors, computer simulation of the resulting spacecraft motion can be complex, requiring extensive reprogramming for each case considered. A graphical technique is described in this Note which permits rapid evaluation of the effects of a stepping sensor on the motion of the basic spacecraft.

### Basic Gimbaled Appendage Motions

The dynamic system used to illustrate spacecraft response to gimbaled scan sensor perturbations consists of a rotor-stabilized spacecraft with gimbaled appendage (Fig. 1). The vehicle is assumed to have equal transverse moments-of-inertia; i.e., it is symmetric about the spin-axis of the rotor. Gimbaled appendage motion can be categorized in two types: azimuth motions, which are rotations about an axis parallel to the vehicle's spin axis, and elevation motions, which are rotations about a transverse axis. Azimuth motions interact directly with the spin control system of the rotor. Studies of these interactions require detailed simulation of the spin control system. Of more immediate interest here are elevation motions that do not interact with the interbody control loop, except in cases involving product-of-inertia coupling of platform azimuth and nutation motions. Otherwise, the main effect of elevation motions of an articulated appendage is to cause the spacecraft to nutate.

Fig. 1 Spacecraft with gimbaled appendage.

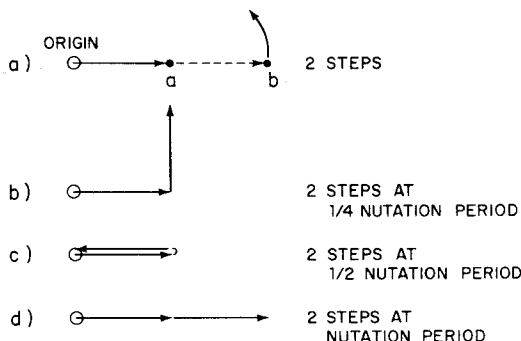
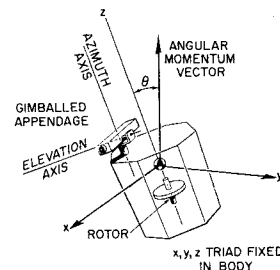


Fig. 2 Nutation step sequences.

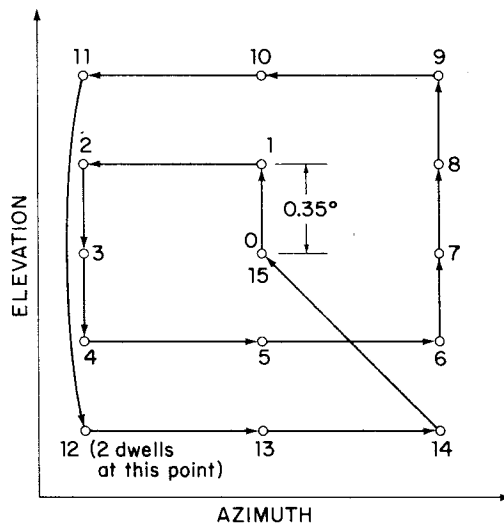


Fig. 3 Search scan pattern.

If an appendage, such as the device shown in Fig. 1 is stepped an angle,  $\phi$ , in a very short time (i.e., short compared with the natural nutation period of the spacecraft), it impulsively induces a nutation of the spacecraft. The amount of nutation, measured by nutation angle  $\Theta$  between the spacecraft's spin axis and the angular momentum (Fig. 1) is proportional to the angle  $\phi$ , the constant of proportionality being the ratio of transverse inertias, i.e.,

$$\Theta = (I/J_T)\phi \quad (1)$$

where  $J_T$  is the transverse inertia of the spacecraft, and  $I$  is the transverse inertia of the device. If, after some time, a second elevation step occurs, it induces an additional nutation. However, this change in nutation angle will occur at some phasing relative to the original, since the spacecraft's z-axis will have been coning about the angular momentum vector because of the initial nutation. Thus, analysis of the effects of a series of steps can become complicated.

### Nutation Coordinate System

A convenient method for following spacecraft motions during a sequence of appendage elevation steps has been devised. Essentially a graphic technique, it involves defining a

Received March 28, 1975; revision received May 21, 1975. This work was sponsored by the U.S. Air Force.

Index category: Spacecraft Attitude Dynamics and Control.

\*Staff Member, Member AIAA.

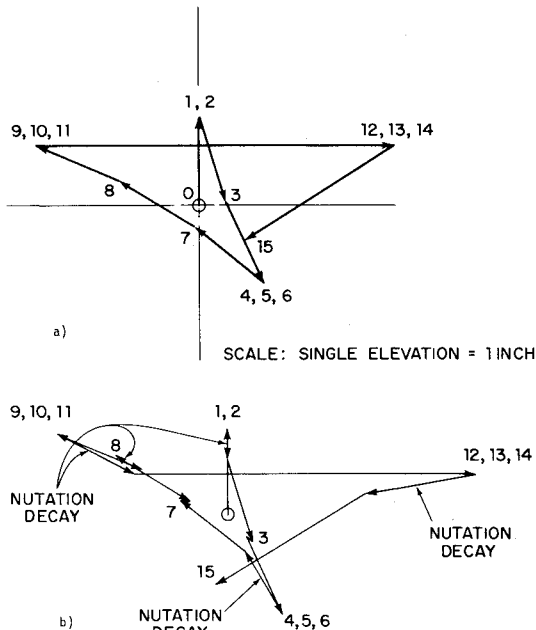


Fig. 4 Nutation angle during a) scan and b) scan with nutation damping.

"nutation coordinate system," which is a plane centered on the angular momentum vector of the spacecraft and rotates at the spacecraft's inertial nutation rate. Because this coordinate system rotates, intersection of the spacecraft's spin axis with the plane is a stationary point (except when a nutation damper is present, which is discussed later) and the distance of this point from the origin is a measure of the nutation angle,  $\Theta$ . By keeping track of the amplitude and phasing of a series of elevation steps, their effect can be plotted on the nutation coordinate system to obtain the finally induced nutation angle.

Assume a spacecraft in pure spin. An appendage elevation step produces a nutation  $\Theta$  which can be represented by a vector in some direction in the nutation coordinate system (Fig. 2a). This moves the point representing the spin axis intersection from the origin (pure spin case) to point *a*. If another appendage elevation step were performed immediately in the same direction, the spin axis would be moved to point *b*. However, if there is a time delay before the second elevation step, then the "potential nutation change vector" will rotate at the nutation rate through some angle. For example, if the second elevation step is performed at one-fourth of the nutation period after the first step, then the potential vector will have rotated one-fourth of a complete revolution resulting in the spin axis movement shown in Fig. 2b. Phasing the second step at 1) one-half the nutation period (Fig. 2c) and 2) equal to the nutation period (or integral multiple thereof) (Fig. 2d), produce similar results. The orientation of a gimbaled appendage can be altered in elevation with no residual spacecraft nutation by performing the re-orientation in two steps, separated by one-half the nutation period, as illustrated in Fig. 2c. Conversely, if an appendage is stepped alternately up and down, phasing these steps at one-half the nutation period tends to build up the nutation.

### Examples

The spiral search pattern (Fig. 3) involves rapid elevation and azimuth steps followed by dwells at each location. The single-step error. The residual error at the end of the scan is three-fourths of the single-step error.

The usefulness of this graphic technique is demonstrated in accounting for nutation decay brought about by a nutation damper. A linear nutation damper mounted on the despun platform reduces the nutation angle of a freely nutating spacecraft exponentially, i.e.,

$$\Theta = \Theta_0 e^{-t/\tau} \quad (2)$$

where  $\tau$  is the "time constant" associated with the nutation damper. In the nutation coordinate system, the point representing the spin axis location moves directly toward the origin at this rate. Hence, the effect of nutation decay on a sequence of elevation steps can be easily accounted for by azimuth steps do not affect spacecraft nutation. Following spacecraft motion via the nutation coordinate system for a search pattern with 3.6-sec dwells, and a spacecraft with nutation period of 160 sec (Fig. 4a), the potential nutation change vector rotates  $(3.6/160) 360^\circ$  or  $8.1^\circ$ , during each dwell. Maximum error during the search is 2.5 times the reducing the radius vector to each point by the appropriate amount, from Eq. (2), before adding the effect of the next step. (This approach neglects transients in the damper's motion.) For example, the system described previously in Fig. 4a can also be analyzed with nutation decay occurring. The time constant in Eq. (2) was assumed to be 18 sec. Then Eq. (2) gave the change in  $\Theta$  as 18% during each dwell. The diagram in Fig. 4a was then redrawn (Fig. 4b) where each radius vector is reduced by the appropriate amount before adding each subsequent step. The maximum error is 2.92 of the single-step nutation error, and the residual error is 0.83 of the single-step error.

This coordinate system representation of elevation steps also permits a straightforward assessment of the general problem; given a set of  $n$  randomly spaced elevation steps of random magnitude, what is the most probable resulting error? The sequence of such random steps produces in a nutation coordinate system the classic "random walk" problem, the solution of which is well known and is

$$e = L(n)^{1/2} \quad (3)$$

where  $e$  is the expected value of the final error,  $L$  the rms average step size, and  $n$  the number of steps.<sup>1</sup>

### Conclusions

In situations involving elevation motions of a gimbaled appendage, or pulsing of an axially aligned attitude control pulser, those motions that are in resonance with the nutation frequency of the spacecraft can build up the precession or nutation angle of the vehicle very rapidly. Hence, such phasing of the perturbations ought to be avoided if spacecraft pointing accuracy is to be maintained. The nutation coordinate system provides the analyst with a "tool" for rapid evaluation of spacecraft response to this class of disturbances.

### Reference

- 1 Gamow, G., *One, Two, Three - Infinity*, New American Library, New York, 1947, pp. 191-194.